Leveraging AutoML and Deep Learning for Object-Based LULC Classification from Multispectral UAV Imagery

Ilyas Aydin[1], Umut Gunes Sefercik[1], Ali Hosingholizade[2*]

[1]Gebze Technical University, Faculty of Engineering, Dept. of Geomatics Engineering, Kocaeli, Türkiye - ilyasaydin@gtu.edu.tr, sefercik@gtu.edu.tr
[2]University of Tehran, Faculty of Geography, Dept. of Remote Sensing and GIS, Tehran, Iran - a.hosingholizade@ut.ac.ir

Keywords: MS UAV, CNN, XGBoost, AutoGluon, LULC, NDSM

Abstract

Accurate and timely Land Use and Land Cover (LULC) mapping plays a crucial role in various applications, including environmental monitoring, natural resource management, and urban planning. Although satellite imagery continues to serve as a valuable tool for regional-scale analyses, its inherent spatial and temporal constraints often impede the realization of detailed classification tasks. Unmanned Aerial Vehicles (UAVs) equipped with multispectral (MS) sensors offer a cost-effective, high-resolution alternative, enabling the acquisition of fine-scale spatial heterogeneity. This study proposes an object-based LULC mapping approach using MS UAV imagery and advanced machine learning and deep learning algorithms to enhance classification accuracy. Three models, Extreme Gradient Boosting (XGBoost), Convolutional Neural Networks (CNN), and AutoGluon, were implemented to evaluate their performance in multi-class LULC classification. A high-precision Normalized Digital Surface Model (NDSM) was generated through photogrammetric processing and combined with 68 object-level features, including spectral indices, geometric, and texture attributes. Based on F1 scores, XGBoost outperformed the other models with a score of 0.95, followed closely by AutoGluon (0.93) and CNN (0.92), confirming the strong effectiveness of tree-based ensemble methods for LULC classification tasks. Although AutoGluon exhibited slightly lower accuracy, its user-friendly interface, automatic model selection, and minimal manual parameter tuning requirements rendered it an accessible framework for efficient LULC classification. The findings indicate that the integration of MS UAV-based imagery with AutoML and deep learning techniques facilitates high-quality mapping in complex landscapes. The incorporation of NDSM data further augmented classification performance, enhancing accuracy by 8 to 11% for concrete roofs and approximately 8% for roads.

1. Introduction

Land use and land cover (LULC) represent essential aspects of the Earth's system, closely linked to both natural processes and human activities across environmental domains (Detsikas et al., 2024). Accurate and up-to-date LULC information serves as a critical foundation for numerous applications, including natural resource management (Nikolakopoulos and Petropoulos, 2025), urban planning (Kalantar et al., 2017), environmental assessment (Kilic et al., 2006), sustainable development (Arifeen et al., 2021), disaster response (Sheykhmousa et al., 2019), and climate change studies (Olivares et al., 2019). LULC data provides spatially explicit insights into how land is utilized and transformed over time, serving as a crucial foundation for monitoring environmental change and managing natural resources.

In recent decades, remote sensing has revolutionized land monitoring and LULC classification by providing a more efficient alternative to traditional field-based methods often time-consuming and labour-intensive. Although satellites provide the advantage of wide area coverage and revisit capabilities, they face inherent limitations in spatial and temporal resolution when high-level of detail analysis is required. This often results in challenges for detecting small objects or producing precise, localized maps (Park et al., 2022). Additionally, factors such as cloud cover further restrict the usability of satellite imagery in certain conditions. Unmanned aerial vehicles (UAVs) have emerged as a powerful alternative remote sensing tool to overcome such difficulties in LULC mapping. By providing very high-resolution multispectral (MS) data from lower flight altitudes, UAVs overcome many limitations of traditional satellite imagery, including issues related to spatial resolution and cloud cover interference. Equipped with advanced sensor technologies, autonomous flight capabilities, and real-time data acquisition systems (Delavarpour et al., 2021; Silva et al., 2019), UAVs enable flexible and efficient data collection even in localized or difficult to access areas. Furthermore, their compatibility with user-friendly software interfaces enhances their accessibility and practicality for a wide range of users. These advantages make UAV-based imagery particularly valuable for detailed environmental monitoring, precision mapping, and timely decision making processes.

Although VHR imagery offers detailed spatial information, it also introduces challenges for land cover classification. Spectrally similar classes, especially in complex areas like forests or cities, can be hard to distinguish (Detsikas et al., 2024; Gibril et al., 2020). Pixel-based methods often ignore spatial context, leading to issues such as the salt-and-pepper effect. UAVs with only RGB sensors may lack sufficient spectral details, and large data volumes from VHR images can make photogrammetric processing more difficult (Puniach et al., 2024). In this context, over the last two decades, numerous classification approaches have been introduced to extract land cover features from UAV images, and object-based image analysis (OBIA) has emerged as the widely adopted method in recent studies (Kalantar et al., 2017).

In this study, an object-based LULC mapping approach was conducted using MS UAV imagery and a precise Normalized

* Corresponding author

Digital Surface Model (NDSM) derived from the same data, aiming to overcome the limitations of reduced class separability caused by restricted spectral information. Two distinct datasets were developed based on spectral, index-based, geometric, and textural features, following the methodology of Aydın and Sefercik (2025). One dataset included NDSM data to enhance vertical feature differentiation, while the other excluded height information. Both datasets were systematically evaluated using Extreme Gradient Boosting (XGBoost), AutoGluon, and Convolutional Neural Network (CNN) models. The heterogeneous nature of the study area, consisting of 11 distinct LULC classes, positively contributed to the generalization of the results and enabled a more robust assessment of the effectiveness of MS UAVs in LULC mapping applications. Among the tested approaches, AutoGluon is a relatively user-friendly and easy-to-deploy AutoML framework, but its actual performance in the context of LULC classification has not yet been extensively investigated in the literature before this work. The results demonstrated that the integration of MS UAV data with the AutoGluon classifier can enable high-accuracy LULC mapping applications. However, when overall model performance is considered, the XGBoost algorithm achieved the highest classification accuracy among the tested methods.

2. Study Area and Materials

The study area is located in the northern part of the Gebze Technical University campus, within the Gebze district of Kocaeli province, Türkiye, and adjacent to the Sea of Marmara (Figure 1). The terrain is generally flat and the orthometric elevation is approximately 10 m. The area covers nearly 36 ha, including a rich diversity of LULC classes such as concrete roof, red roof, coniferous tree, broadleaved tree, road, soil, water, low vegetation, grass, shadow, and bicycle path. The vegetation is predominantly composed of species like Stone pine, Calabrian pine, Plane tree, and Black poplar, offering a broad spectrum of spectral and structural characteristics. This variety supports detailed analysis of LULC classification performance, particularly within complex, multi-class settings.

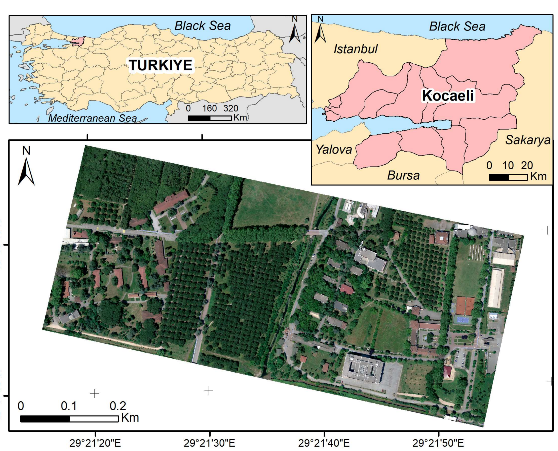

Figure 1. Location of study area.

Aerial data acquisition was conducted using the DJI Phantom IV MS UAV, equipped with six cameras capable of simultaneously capturing red, green, blue, red edge, near-infrared (NIR), and RGB composite images. The UAV's real-time kinematic (RTK) GNSS module enables high positional accuracy for photogrammetric outputs without requiring ground control points (GCPs). However, to ensure absolute orientation accuracy in the event of RTK interruptions, eight mobile polycarbonate GCPs (0.25 m × 1 m) were deployed and georeferenced using a CHC-i80 GNSS receiver via the Network-RTK method. The captured UAV images were radiometrically calibrated using a MAPIR V2 target with four independent colors: black, dark gray, light gray, and white whose reflectance values were determined under laboratory conditions. The integration of additional spectral bands, especially red edge and NIR, greatly enhanced vegetation discrimination capabilities and improved classification performance, underscoring the suitability of MS UAV systems for detailed environmental monitoring tasks.

3. Methodology

This study adopts a structured and integrated methodology to ensure the production of high-quality LULC maps from UAV-based MS data. The overall workflow encompasses several key stages: initial field reconnaissance, establishment of GCPs, flight planning and aerial image acquisition, photogrammetric processing, LULC classification, and accuracy assessment of the final outputs (Figure 2).

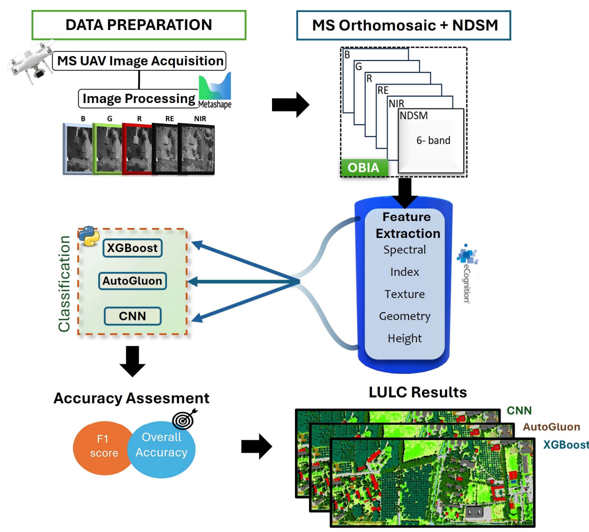

Figure 2. Workflow of the study.

3.1 Image Acquisition and Data Processing

The flight planning and all parameter settings for the acquisition of aerial images were managed via the DJI Ground Station Pro (GS Pro) application. A flight altitude of 110 m was preferred to achieve a ground sampling distance (GSD) of approximately 0.06 m considering the required spatial resolution and operational safety. To ensure full coverage of the study area, the flight path was designed with 80% front and 60% side overlap. Due to the UAV's battery limitations, data acquisition was completed in two consecutive flights lasting a total of approximately 40 minutes. Image capturing was conducted around noon to minimize shadow effects caused by buildings and vegetation, under optimal lighting conditions. The UAV camera was oriented in nadir position (90°) to record accurate reflectance data. Each capture generated six separate images per shot—one in JPEG format (RGB composite) and five in TIFF—covering all spectral bands. The entire study area was imaged with at least nine overlapping aerial photos per location, resulting in a total of 4,208 images collected over both flights.

The UAV images were photogrammetrically processed using Structure-from-Motion (SfM)-based Agisoft Metashape Pro software. In addition to the standard photogrammetric workflow, supplementary radiometric correction procedures were applied due to the use of MS images captured by different sensors. As a result, an orthomosaic with high radiometric accuracy was produced (Figure 3).

In LULC classification studies, accurate elevation data plays an important role in increasing object differentiation using vertical information (Aydin and Sefercik, 2025). In this study, an NDSM was produced and used as an important feature to increase the classification accuracy by including vertical object information. An NDSM is calculated by extracting the DTM from the DSM in a common area (Hashemi, 2008). In order to produce the highest quality DSM and DTM, point clouds produced in Agisoft Metashape software were transferred to the Microstation Terrascan module, which offers much more comprehensive features in filtering processes. In the Terrascan module, firstly, a point cloud covering all LULC classes was filtered, and cloud used in DSM production was obtained. Then, the cloud used in DTM production was achieved by using only ground points. 10 cm grid DSM and DTM were generated from the regulated point clouds using Surfer software. While the data metrics interpolation method, which allows maximum Z usage, and a 5 m search radius were used in DSM generation, the linear triangulation interpolation method and a 10 m search radius (due to the smaller number of points) were preferred for the DTM. The horizontal offsets of the generated DSM and DTM were eliminated by horizontal shifting method using the BLUH software, and after ensuring 100% horizontal overlap, a 10 cm grid NDSM was produced in the LISA software (Figure 3).

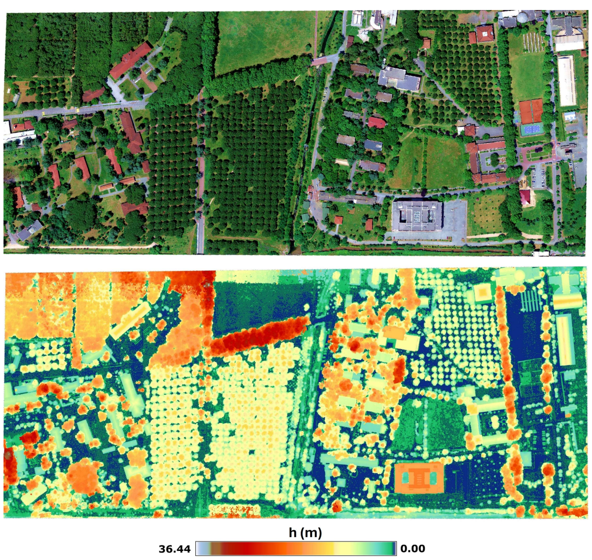

Figure 3. MS Orthomosaic (top) and NDSM (bottom).

3.2. Image Segmentation

In OBIA, the initial step involves the consistent grouping of pixels that exhibit similar spectral characteristics. This approach significantly reduces the processing burden associated with pixel-based methods by shifting the analysis from individual pixels to spatially coherent image objects, thereby incorporating the spatial context and neighbourhood relationships among pixels. To derive image segments with high internal homogeneity and low inter-object heterogeneity, crucial for accurate classification, the widely adopted Multiresolution Segmentation (MRS) algorithm was employed, as implemented in the eCognition Developer software environment.

Prior to segmentation, the NDSM was stacked as an additional band to the MS orthomosaic. This integration enhanced both the consistency and precision of the segmentation, particularly improving delineation at complex structures such as roof edges. To ensure spatial alignment between the datasets, a co-resolution of 10 cm was used during preprocessing, maximizing geometric coherence across the image layers.

The MRS algorithm operates by initially assigning each pixel to a unique image object. It then iteratively merges neighbouring objects based on a homogeneity criterion, continuing this process until the threshold defined by the user is met (Baatz and Schape, 2000; Chen et al., 2009). The segmentation process is governed by three main parameters: scale, shape, and compactness. These parameters critically influence the resulting object boundaries and the overall quality of segmentation. To determine the optimal parameter values, both the ESP-2 (Estimation of Scale Parameter) tool and a trial-and-error approach were utilized, allowing for a balance between over-segmentation and under-segmentation, tailored to the specific characteristics of the study area. A scale parameter of 60 was used for the segmentation, with shape and compactness values set to 0.6 and 0.4, respectively.

Based on the spectral, index-based, textural, and geometric characteristics of the generated segments, a total of 68 features were extracted (Aydin and Sefercik, 2025). In addition to these, elevation information derived from the high-precision NDSM was also incorporated as a feature. All extracted features associated with each segment were compiled into a structured tabular dataset for subsequent analysis.

3.3. LULC Mapping

As aforementioned, the LULC mapping performance of three different classification approaches namely XGBoost, CNN, and AutoGluon, was evaluated. For training data preparation, representative segment samples for each LULC class were carefully selected using the high-resolution orthomosaic. All classification models were trained using a dataset split, with 80% allocated for training and 20% reserved for testing.

To evaluate the influence of elevation information on classification performance, two distinct datasets were constructed: Dataset 1 (D1) excluded the relative elevation derived from the NDSM, while Dataset 2 (D2) incorporated it. This allowed for a detailed analysis of the impact of elevation data on classification performance, both at the class level and classifier level.

XGBoost is a powerful supervised machine learning algorithm that builds on gradient boosting by introducing improvements in model regularization and optimization, making it highly effective across diverse classification tasks (Chen and Guestrin, 2016). It sequentially constructs weak decision trees, where each tree corrects the errors of its predecessor by giving more focus to misclassified instances (Budholiya et al., 2022). The final model aggregates all previous iterations, leading to robust performance (Georganos et al., 2018). XGBoost also incorporates an objective function combining training loss with regularization (Chen et al., 2015), and predictions from individual trees are computed in parallel and then merged (Yao et al., 2022). Despite mechanisms like subsampling to mitigate overfitting, optimal parameter tuning, such as the number of iterations, tree depth, and learning rate is critical to ensure classification accuracy (Budholiya et al.,

https://doi.org/10.5194/isprs-annals-X-4-W8-2025-115-2026 |

2022). In this study, parameter optimization was performed using GridSearchCV to ensure optimal model performance.

While CNNs are well known for their success in per-pixel image classification, they often result in a salt-and-pepper effect and blurred boundaries due to pooling operations (Kucharczyk et al., 2020). To address this, some studies have combined CNNs with GEOBIA to integrate deep features with spatial and spectral information, though challenges remain in handling irregularly shaped objects and merging CNN outputs with object-based features (Hossain and Chen, 2024; Jozdani et al., 2019). In contrast, tabular deep learning models operate directly on structured data, where each row represents a segment and each column an extracted feature. These models, including differentiable trees and attention-based architectures, have shown superior performance compared to shallow classifiers on tabular data (Gorishniy et al., 2021; Popov et al., 2020). Although CNNs are not inherently designed for tabular data, a 1D CNN can be adapted by reshaping feature vectors into sequences, allowing convolutional layers to capture local interactions across features. In this study, a 1D CNN was implemented on tabular segment-level data to classify segmented data based on extracted features and to leverage its feature-learning capability within the GEOBIA framework. The model architecture consists of two convolutional layers with ReLU activation, each followed by batch normalization and max pooling layers to reduce dimensionality and improve generalization. The convolutional blocks are followed by a flattening layer and two fully connected dense layers with ReLU activation, batch normalization, and dropout regularization to prevent overfitting. The final output layer uses softmax activation for multi-class classification. The model was compiled with the Adam optimizer and trained using categorical cross-entropy loss. An early stopping mechanism was employed to halt training when validation loss stopped improving, ensuring optimal model performance.

AutoGluon-Tabular is an AutoML framework designed for structured data, enabling high-accuracy model training with minimal code. Unlike traditional AutoML tools focused on exhaustive model selection, it emphasizes multi-layer stacking and repeated k-fold bagging to boost performance. It automatically performs data preprocessing, identifies the prediction task, and trains a diverse set of models, including neural networks, gradient boosted trees (e.g., LightGBM and CatBoost), and classical machine learning algorithms. These models are strategically ensembled to improve robustness. AutoGluon offers fast, scalable training and has shown superior accuracy and efficiency compared to other AutoML platforms in extensive benchmarks (Erickson et al., 2020). In this study, it was used in a classification task based on tabular data. AutoGluon builds a stack ensemble model, where the predictions of multiple base models are used as additional features for higher-level models. This layered approach, known as stack ensembling, improves robustness and accuracy by combining the strengths of diverse algorithms. The final output is generated by a weighted ensemble model, which optimally combines predictions from all layers. In this study, AutoGluon was utilized with its default stack ensembling strategy to automatically train and select the best-performing models.

3.4. Accuracy Assessment

For the accuracy assessment of the thematic maps produced by the three different approaches mentioned previously, a high-resolution orthomosaic (6 cm) was used as the base reference layer. Reference polygons were manually delineated for each LULC class to serve as ground truth data. Using these reference polygons, confusion matrices were generated, and key performance metrics including precision, recall, F1 score, and overall accuracy (OA) were computed to evaluate the classification results (1–3). In this context, TP, TN, FP, and FN refer to true positives, true negatives, false positives, and false negatives, respectively. The accuracy assessments were conducted using the Semi-Automatic Classification Plugin (SCP) within the QGIS software environment (Congedo, 2017), which provides integrated tools for post-classification validation and metric calculation.

$$P = TP/(TP + FP) \tag{1}$$

$$R = TP/(TP + FN) \tag{2}$$

$$F1 = 2 \times (P \times R)/(P + R) \tag{3}$$

4. Results and Discussion

The analysis revealed that, across all classifiers, the inclusion of relative height information (NDSM – D2) led to a decrease in F1 scores for the water and bicycle path classes (Figure 4). Detailed visual and statistical assessments showed that the addition of elevation data disrupted the balance between elevation-consistent surfaces. For instance, ground-level areas with similar spectral characteristics (e.g., blue hues) were often misclassified as water, and roads at the same elevation as bicycle paths led to misclassification.

On the other hand, the inclusion of height information significantly improved the classification performance of concrete roof and road classes across all models. Conversely, classes such as red roof, coniferous tree, and broad-leaved tree exhibited high separability even in the absence of elevation data (D1), allowing for accurate classification based solely on spectral, textural, and geometric features. When evaluating overall performance, the lowest classification accuracy was observed in the low vegetation class, which represents sparse vegetation, and the bicycle path class, which had limited representation in the training data due to its small spatial coverage in the study area. The limited number of training samples for the bicycle path class particularly affected the performance of deep learning models that require a large amount of data.

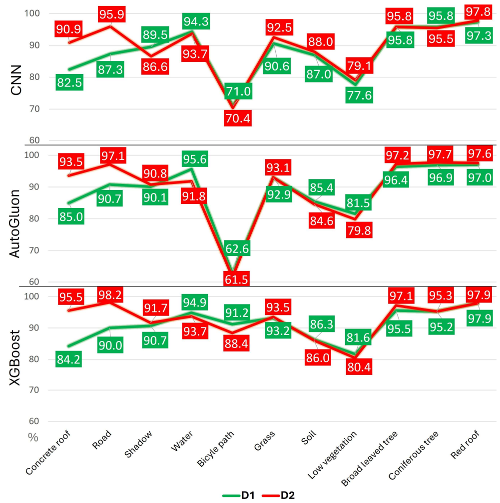

Figure 4. Comparison of class-level F1 scores by classifier and dataset in LULC mapping.

In contrast, this issue was not observed in the tree-based XGBoost model, which showed greater robustness to imbalanced data. The inclusion of elevation data improved the classification accuracy of the concrete roof class by 8 to 11% and the road class by approximately 8% across all classifiers.

Figure 5 presents a high-resolution orthomosaic image of a sample building classified as a concrete roof, along with a comparative visualization of the LULC thematic maps generated using classifiers for both datasets. Visual analysis revealed that in the absence of elevation information (D1), the building roof was largely confused with the road class, leading to significant misclassification. In contrast, the inclusion of elevation data (D2) significantly improved classification accuracy across all methods.

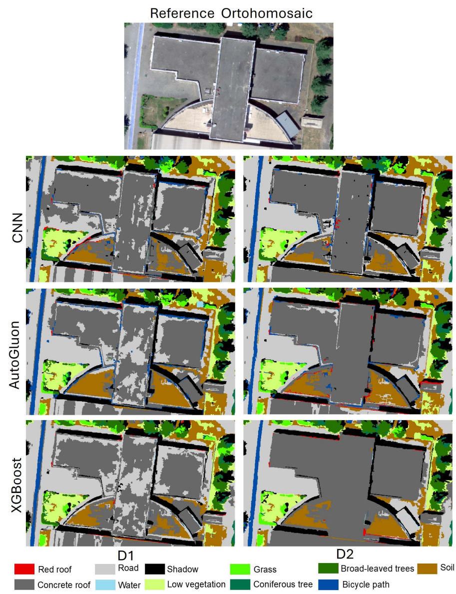

Figure 5. Comparative thematic maps generated by CNN, AutoGluon, and XGBoost for a concrete roofed building across different datasets.

The LULC thematic map generated using the highest-performing XGBoost model and the D2 dataset is presented in Figure 6.

Figure 6. LULC map generated by XGBoost for D2 dataset.

The comparative evaluation of CNN, AutoGluon, and XGBoost models on two different datasets (D1 and D2) for LULC classification reveals significant performance differences influenced by the presence of elevation information. Across all models, the inclusion of elevation data (D2) led to substantial performance improvements (Figure 7). XGBoost yielded the highest performance, achieving an F1-score of 94.52% and an OA of 94.65% on D2. AutoGluon also performed strongly, particularly on D2 (F1-score: 93.39%, OA: 93.62%), outperforming the CNN in both datasets. Notably, CNN exhibited lower accuracy, especially on D1, where its F1-score and OA remained below 89%. These findings underscore the value of elevation information in enhancing classification performance and demonstrate the superiority of ensemble and automated learning approaches over traditional deep learning architectures in this context. NDSM has been particularly effective in solving common misclassification problems between flat, man-made surfaces with similar spectral responses.

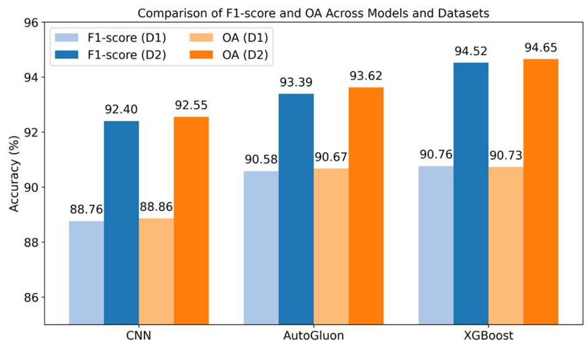

Figure 7. Performance comparison of CNN, AutoGluon, and XGBoost models based on F1-score and overall accuracy for D1 and D2.

5. Conclusion

This study aimed to evaluate the effectiveness of different machine learning and deep learning methods in object-based LULC classification of MS UAV orthomosaics by testing different feature combinations and model types. In this context, three different algorithms, namely CNN, AutoGluon, and XGBoost, were comparatively evaluated across two datasets: one without elevation information (D1) and one incorporating a high-quality NDSM (D2). The inclusion of the NDSM in D2 significantly improved classification performance, particularly by facilitating the separation of spectrally similar classes such as roads and concrete roofs.

Among the tested models, the tree-based ensemble algorithm XGBoost consistently demonstrated the highest classification performance. Specifically, the model trained on D2 achieved the highest OA (94.65%) and F1-score (94.52%), outperforming both the deep learning-based CNN and the AutoML-based AutoGluon. While CNN underperformed in comparison, AutoGluon delivered promising results with strong generalization capability, offering a practical solution for users with limited experience in manual model tuning. This study highlights the high potential of MS UAV imagery combined with automated ML approaches and height-based features for producing accurate LULC maps. The ease of use and reliable performance of AutoGluon make it a valuable tool in complex classification tasks. Future studies can explore the effectiveness of this approach across different landscapes and land cover types to enhance its general applicability.

References

Arifeen, H.M., Phoungthong, K., Mostafaeipour, A., Yuangyai, N., Yuangyai, C., Techato, K., Jutidamrongphan, W., 2021~~.~~: Determine the land-use land-cover changes, urban expansion and their driving factors for sustainable development in gazipur Bangladesh. Atmosphere (Basel) 12. https://doi.org/10.3390/atmos12101353

Aydin, I., Sefercik, U.G., 2025~~.~~: Multispectral UAV-based LULC mapping performance improvement by integrating precise NDSM data and machine learning algorithms. Earth Sci Inform 18, 326. https://doi.org/10.1007/s12145-025-01841-w

Baatz, M., Schape, A., 2000~~.~~: Multiresolution segmentation - An optimization approach for high quality multi-scale image segmentation angewandte geographische informationsverarbeitung XII. Proceedings of Angewandte Geographische Informations Verarbeitung XII.

Budholiya, K., Shrivastava, S.K., Sharma, V., 2022~~.~~: An optimized XGBoost based diagnostic system for effective prediction of heart disease. Journal of King Saud University - Computer and Information Sciences 34, 4514–4523. https://doi.org/10.1016/j.jksuci.2020.10.013

Chen, J., Pan, D., Mao, Z., 2009~~.~~: Image-object detectable in multiscale analysis on high-resolution remotely sensed imagery. Int J Remote Sens 30, 3585–3602. https://doi.org/10.1080/01431160802585348

Chen, T., Guestrin, C., 2016~~.~~: XGBoost, in: Proceedings of the 22nd ACM SIGKDD International Conference on Knowledge Discovery and Data Mining. ACM, New York, NY, USA, pp. 785–794. https://doi.org/10.1145/2939672.2939785

Chen, T., He, T., Benesty, M., Khotilovich, V., Tang, Y., Cho, H., Zhou, T., 2015~~.~~: XGBoost : eXtreme Gradient Boosting. R package version 0.71-2.

Congedo, L., 2017~~.~~: Semi-Automatic Classification Plugin Semi-Automatic Classification Plugin Documentation. Scp.

Delavarpour, N., Koparan, C., Nowatzki, J., Bajwa, S., Sun, X., 2021~~.~~: A Technical Study on UAV Characteristics for Precision Agriculture Applications and Associated Practical Challenges. Remote Sens (Basel) 13, 1204. https://doi.org/10.3390/rs13061204

Detsikas, S.E., Petropoulos, G.P., Kalogeropoulos, K., Faraslis, I., 2024~~.~~: Combining Low-Cost UAV Imagery with Machine Learning Classifiers for Accurate Land Use/Land Cover Mapping. Earth (Switzerland) 5, 244–254. https://doi.org/10.3390/earth5020013

Erickson, N., Mueller, J., Shirkov, A., Zhang, H., Larroy, P., Li, M., & Smola, A.~~, (~~2020~~).~~: Autogluon-tabular: Robust and accurate automl for structured data. arXiv preprint arXiv:2003.06505.

Georganos, S., Grippa, T., Vanhuysse, S., Lennert, M., Shimoni, M., Wolff, E., 2018~~.~~: Very High Resolution Object-Based Land Use–Land Cover Urban Classification Using Extreme Gradient Boosting. IEEE Geoscience and Remote Sensing Letters 15, 607–611. https://doi.org/10.1109/LGRS.2018.2803259

Gibril, M.B.A., Kalantar, B., Al-Ruzouq, R., Ueda, N., Saeidi, V., Shanableh, A., Mansor, S., Shafri, H.Z.M., 2020~~.~~: Mapping heterogeneous urban landscapes from the fusion of digital surface model and unmanned aerial vehicle-based images using adaptive multiscale image segmentation and classification. Remote Sens (Basel) 12. https://doi.org/10.3390/rs12071081

Gorishniy, Y., Rubachev, I., Khrulkov, V., Babenko, A., 2021~~.~~: Revisiting Deep Learning Models for Tabular Data, in: Advances in Neural Information Processing Systems.

Hashemi, S.A.M., 2008~~.~~: Automatic peaks extraction from Normalized Digital Surface Model (NDSM). isprs.org.

Hossain, M.D., Chen, D., 2024~~.~~: Performance Comparison of Deep Learning (DL)-Based Tabular Models for Building Mapping Using High-Resolution Red, Green, and Blue Imagery and the Geographic Object-Based Image Analysis Framework. Remote Sens (Basel) 16. https://doi.org/10.3390/rs16050878

Jozdani, S.E., Johnson, B.A., Chen, D., 2019~~.~~: Comparing deep neural networks, ensemble classifiers, and support vector machine algorithms for object-based urban land use/land cover classification. Remote Sens (Basel) 11. https://doi.org/10.3390/rs11141713

Kalantar, B., Mansor, S. Bin, Sameen, M.I., Pradhan, B., Shafri, H.Z.M., 2017~~.~~: Drone-based land-cover mapping using a fuzzy unordered rule induction algorithm integrated into object-based image analysis. Int J Remote Sens 38, 2535–2556. https://doi.org/10.1080/01431161.2016.1277043

Kilic, S., Evrendilek, F., Berberoglu, S., Demirkesen, A.C., 2006~~.~~: Environmental monitoring of land-use and land-cover changes in a Mediterranean Region of Turkey. Environ Monit Assess 114. https://doi.org/10.1007/s10661-006-2525-z

Kucharczyk, M., Hay, G.J., Ghaffarian, S., Hugenholtz, C.H., 2020~~.~~: Geographic object-based image analysis: A primer and future directions. Remote Sens (Basel). https://doi.org/10.3390/rs12122012

Nikolakopoulos, I.A., Petropoulos, G.P., 2025~~.~~: Obtaining a Land Use/Cover Cartography in a Typical Mediterranean Agricultural Field Combining Unmanned Aerial Vehicle Data with Supervised Classifiers. Land (Basel) 14. https://doi.org/10.3390/land14030643

Olivares, E.A.O., Torres, S.S., Jiménez, S.I.B., Enríquez, J.O.C., Zignol, F., Reygadas, Y., Tiefenbacher, J.P., 2019~~.~~: Climate change, land use/land cover change, and population growth as drivers of groundwater depletion in the Central Valleys, Oaxaca, Mexico. Remote Sens (Basel) 11. https://doi.org/10.3390/rs11111290

Park, G., Park, K., Song, B., Lee, H., 2022~~.~~: Analyzing Impact of Types of UAV-Derived Images on the Object-Based Classification of Land Cover in an Urban Area. Drones 6, 71. https://doi.org/10.3390/drones6030071

Popov, S., Morozov, S., Babenko, A., 2020~~.~~: NEURAL OBLIVIOUS DECISION ENSEMBLES FOR DEEP LEARNING ON TABULAR DATA, in: 8th International Conference on Learning Representations, ICLR 2020.

Puniach, E., Gruszczyński, W., Ćwiąkała, P., Strząbała, K., Pastucha, E., 2024~~.~~: Recognition of Urbanized Areas in UAV-Derived Very-High-Resolution Visible-Light Imagery. Remote Sens (Basel) 16. https://doi.org/10.3390/rs16183444

Sheykhmousa, M., Kerle, N., Kuffer, M., Ghaffarian, S., 2019~~.~~: Post-disaster recovery assessment with machine learning-derived land cover and land use information. Remote Sens (Basel) 11. https://doi.org/10.3390/rs11101174

Silva, L. de O., Bandeira, R.A. de M., Campos, V.B.G., 2019~~.~~: Proposal to planning facility location using UAV and geographic information systems in a post-disaster scenario. International Journal of Disaster Risk Reduction 36, 101080. https://doi.org/10.1016/j.ijdrr.2019.101080

Yao, X., Fu, X., Zong, C., 2022~~.~~: Short-Term Load Forecasting Method Based on Feature Preference Strategy and LightGBM-XGboost. IEEE Access 10, 75257–75268. https://doi.org/10.1109/ACCESS.2022.3192011